

Clock-transition spectrum of ^{171}Yb atoms in a one-dimensional optical lattice*

Chen Ning(陈宁), Zhou Min(周敏), Chen Hai-Qin(陈海琴), Fang Su(方苏),
Huang Liang-Yu(黄良玉), Zhang Xiao-Hang(张晓航), Gao Qi(高琪), Jiang Yan-Yi(蒋燕义),
Bi Zhi-Yi(毕志毅), Ma Long-Sheng(马龙生), and Xu Xin-Ye(徐信业)[†]

State Key Laboratory of Precision Spectroscopy and Department of Physics, East China Normal University, Shanghai 200062, China

(Received 11 March 2013; revised manuscript received 8 April 2013)

An optical atomic clock with ^{171}Yb atoms is devised and tested. By using a two-stage Doppler cooling technique, the ^{171}Yb atoms are cooled down to a temperature of $6 \pm 3 \mu\text{K}$, which is close to the Doppler limit. Then, the cold ^{171}Yb atoms are loaded into a one-dimensional optical lattice with a wavelength of 759 nm in the Lamb–Dicke regime. Furthermore, these cold ^{171}Yb atoms are excited from the ground-state $^1\text{S}_0$ to the excited-state $^3\text{P}_0$ by a clock laser with a wavelength of 578 nm. Finally, the $^1\text{S}_0$ – $^3\text{P}_0$ clock-transition spectrum of these ^{171}Yb atoms is obtained by measuring the dependence of the population of the ground-state $^1\text{S}_0$ upon the clock-laser detuning.

Keywords: optical lattice clocks, laser cooling and trapping, ytterbium, clock-transition spectrum

PACS: 06.30.Ft, 32.30.–r, 37.10.De, 37.10.Jk

DOI: 10.1088/1674-1056/22/9/090601

1. Introduction

Owing to intrinsically having ultranarrow-linewidth optical-frequency transitions, group II atomic species and similar species such as ytterbium may be used in new frequency standards.^[1–8] The research on laser cooling, trapping and applications of such atomic species have been a hot topic in the field of atomic and optical physics. Since having many atoms in each atomic optical clock instead of only one single trapped ion in each ion optical clock, the frequency stability of the atomic optical clocks is theoretically predicted to be better than that of the ion optical clocks. By using the optical lattice technique,^[1] all atoms in an atomic optical clock

are confined in the Lamb–Dicke regime, so that the Doppler shift, recoil shift, and collisional shift of the clock-transition frequency are dramatically reduced. Furthermore, by employing an optical lattice with a special wavelength, the AC Stark shift of the clock transition induced by the lattice light will be minimized. Therefore, the frequency uncertainty of the atomic optical clocks will not be worse than that of the ion optical clocks. However, recent experimental results show that the frequency stability and uncertainty of the best atomic optical clock^[3,4] and the best ion optical clock^[9] are already at the level of better than 10^{-16} . Atomic optical clocks may become the next-generation frequency standards.

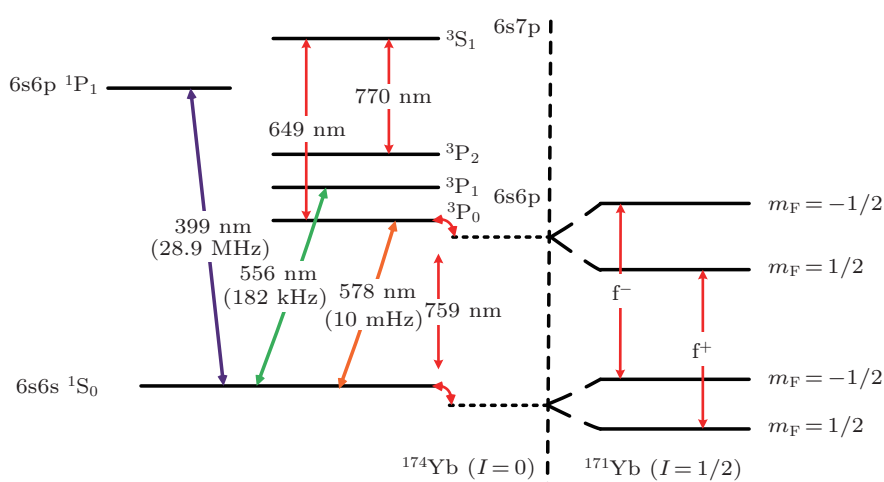


Fig. 1. (color online) Relevant energy levels of ytterbium (^{174}Yb ($I = 0$) and ^{171}Yb ($I = 1/2$)) for laser cooling, trapping, and probing.

*Project supported by the National Basic Research Program of China (Grant Nos. 2012CB821302 and 2010CB922903), the National Natural Science Foundation of China (Grant Nos. 11134003 and 10774044), and the Shanghai Excellent Academic Leaders Program of China (Grant No. 12XD1402400).

[†]Corresponding author. E-mail: xyxu@phy.ecnu.edu.cn

Here we report an experiment on an ytterbium atomic optical clock. Ytterbium has two fermionic isotopes and five bosonic isotopes. Among them, ^{171}Yb ($I = 1/2$) with a natural abundance of 14.3%, ^{173}Yb ($I = 5/2$) with a natural abundance of 16.1%, and ^{174}Yb ($I = 0$) with a natural abundance of 31.8% have been extensively studied. We are mainly interested in ^{171}Yb atoms for their relatively simple energy level structure, which makes them very suitable for application in an atomic clock. Figure 1 shows ytterbium's relevant energy levels for laser cooling, trapping, and probing. In the experiment, by using a 399-nm laser, which corresponds to the strong transition $^1\text{S}_0-^1\text{P}_1$, we first carry out the following experiments: the two-dimensional (2D) optical molasses for collimating the ^{171}Yb atomic beam, Zeeman slowing for decelerating the longitudinal velocity of the ^{171}Yb atomic beam, and laser cooling and trapping ^{171}Yb atoms in the 399-nm magneto-optical trap (MOT). Then by using a narrow-linewidth 556-nm laser, which is related to the weak transition $^1\text{S}_0-^3\text{P}_1$, we further cool the ^{171}Yb atoms in the 556-nm MOT. Furthermore, we load the ultracold ^{171}Yb atoms into a one-dimensional (1D) optical lattice with a wavelength of 759 nm. Finally, by using a cavity-stabilized 578-nm laser, we observe the $^1\text{S}_0-^3\text{P}_0$ clock-transition spectrum of the ^{171}Yb atoms.

2. Experimental details

2.1. Cold-atom preparation

The apparatus of our experiment has been described in detail in Ref. [10]. Here we give a brief description. Because ytterbium atoms have a rather low vapor density at room temperature, we heat them up to 450 °C in a hot oven for vaporization. Then the thermal atomic beam effuses out the hot oven, and is collimated by the 2D optical molasses and decelerated with a Zeeman slower respectively. After that, the ytterbium atoms move into the double MOTs, which are overlapped by a 399-nm MOT and a 556-nm MOT, having a pair of anti-Helmholtz coils and six pairs of counterpropagating laser beams with a $\sigma^+-\sigma^-$ polarization configuration. A schematic diagram is shown in Fig. 2.

The 399-nm laser used for the 2D optical molasses, Zeeman slower, first-stage cooling and probing is an SYST TA-SHG 110 laser system from Toptica, which can provide an output power of 120 mW at 399 nm. We divide the laser power into five parts; besides the four parts mentioned above the other one is used for the frequency stabilization of the 399-nm laser. By using the modulation transfer spectroscopy (MTS) technique,^[11] we can lock the 399-nm laser frequency at the Yb atomic transition for a long time.

After 500 ms of the first-stage cooling in the 399-nm MOT, we measure the temperature of ^{171}Yb atoms by using the time of flight (TOF) method. Using the intensified charge coupled device (ICCD), the images of the atomic cloud are captured at 2 ms or 5 ms after the ^{171}Yb atoms are released from the 399-nm MOT, as shown in Figs. 3(a) and 3(c), respectively. The corresponding spatial distributions along the falling direction are shown in Figs. 3(b) and 3(d) with the fitted curves. The fitting function is $y(x, t) = y_0 + a \exp[-(x - x_0)^2 / r(t)^2]$, where $r(t)$ is the 1/e radius of the cloud. Furthermore, the temperature can be estimated by the following equation: $T = \frac{m}{2k_B} \frac{r(t_2)^2 - r(t_1)^2}{t_2^2 - t_1^2}$, where m is the atomic mass, k_B is the Boltzmann constant, and t is the flight time. As shown in Fig. 3, the measured temperature of the ^{171}Yb atoms is $615 \pm 50 \mu\text{K}$, which is the lowest temperature that we have obtained so far, and it is a little below the Doppler limit of 693 μK in the 399-nm MOT. Typically, the temperature of the ^{171}Yb atoms is about 1 mK with about 10^7 atoms in the 399-nm MOT in our experiment.

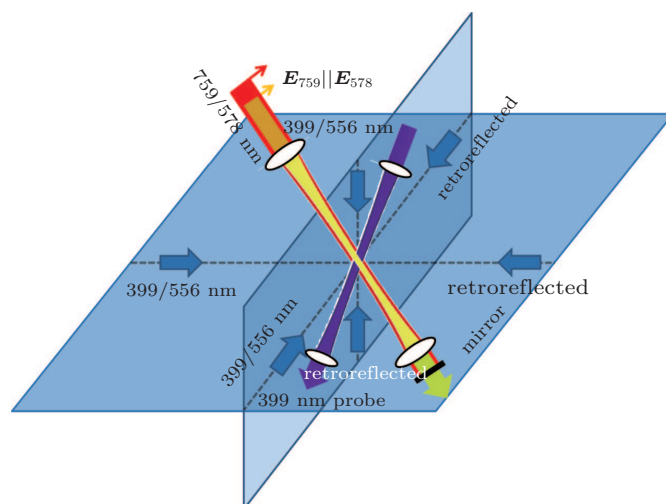


Fig. 2. (color online) Schematic diagram of laser cooling, trapping, and probing of ytterbium atoms. The 399 (556) nm light is used for the first (second) stage cooling. The 759-nm light is used to form the optical lattice. The mirror is used for the 759-nm laser to form a standing wave. The 578-nm light is used to excite ytterbium atoms at the clock transition. The lattice laser and clock laser have the same polarization direction and overlap onto the cold atomic cloud. The 399-nm probe laser is used for measuring the ground-state population.

The 556-nm laser for the second-stage cooling consists of a 1111.6-nm diode laser, a fiber amplifier, and a home-made frequency-doubling system.^[12] The 1111.6-nm laser is first amplified by a fiber optical amplifier, and then enters the single-pass frequency-doubling system. The output power of the 556-nm laser is about 28 mW. The laser is divided into two parts. One, about 600 μW , is used for frequency locking, and the beam interacts orthogonally with the ytterbium atomic beam. By using a photomultiplier tube (PMT), the

fluorescence signal is collected, so that the 556-nm laser frequency is locked to the $^1S_0-^3P_1$ transition of the Yb atoms. The other, with most of the power, is used for the second-stage laser cooling. The laser beam is separated into three parts

by a polarization beam splitter (PBS), and the three parts are overlapped with the 399-nm cooling lasers by using a dichroic mirror (DM) before entering the MOT window, respectively, as shown in Fig. 2.

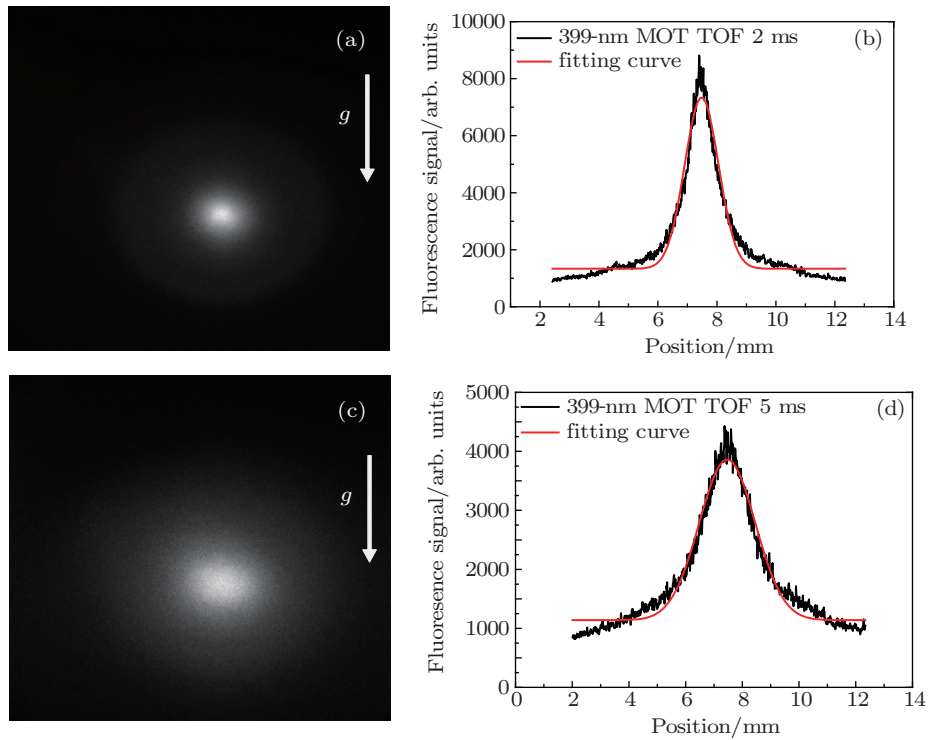


Fig. 3. (color online) The TOF signals of ^{171}Yb atoms released from the 399-nm MOT. (a) and (c) Images of the atomic cloud corresponding to the flight time of 2 ms and 5 ms, respectively, where the arrows represent the direction of gravity. (b) and (d) Corresponding spatial distributions along the falling direction with the fitted curves.

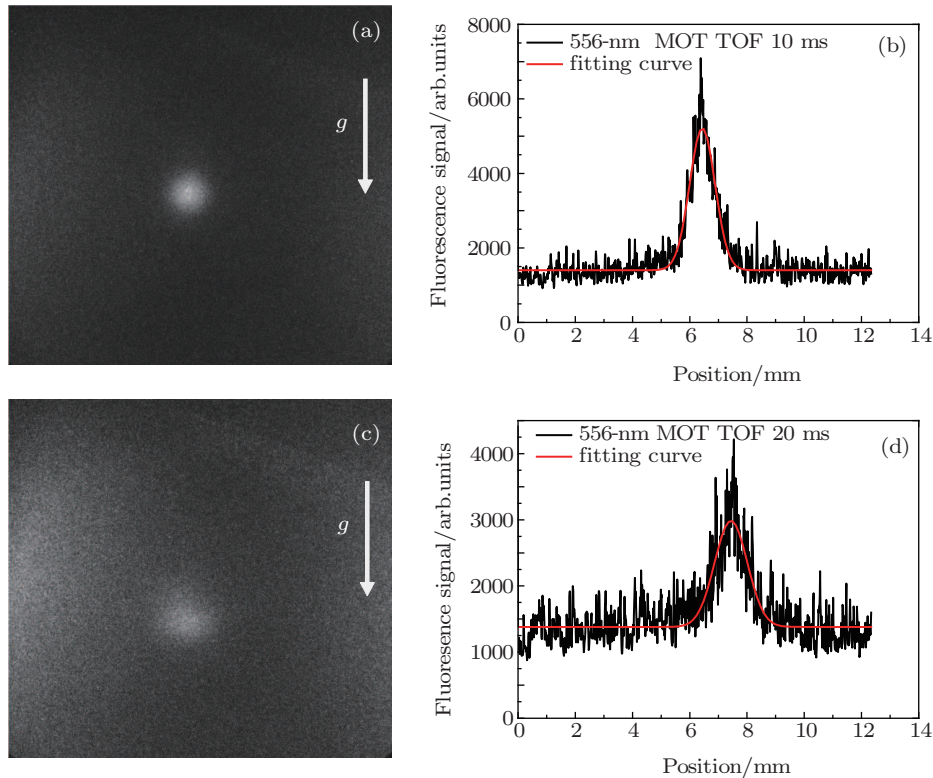


Fig. 4. (color online) The TOF signals of ^{171}Yb atoms. (a) and (c) Images at the flight time of 10 ms and 20 ms after the 556-nm MOT off, respectively. (b) and (d) Corresponding spatial distributions along the falling direction and the fitted curves.

After the 399-nm MOT is turned off, the 556-nm MOT is immediately turned on. The magnetic-field gradient is decreased from 50 G/cm to 15 G/cm simultaneously. The transfer efficiency is about 50%, and about 10^6 atoms are trapped in the 556-nm MOT. In order to obtain a lower temperature, we have optimized the 556-nm laser detuning, the B -field parameters, and so on. After the optimization, the lowest temperature of the ^{171}Yb atoms is about $6 \pm 3 \mu\text{K}$ (the Doppler limit of the second-stage cooling is about $4 \mu\text{K}$.) Figure 4 shows the TOF signals of the ^{171}Yb atoms at 10 ms and 20 ms after being released from the 556-nm MOT, with the fitting results.

2.2. Optical lattice

After the second-stage cooling in the 556-nm MOT, the ultracold Yb atoms are loaded into an optical lattice. Since the atoms are located in the Lamb–Dicke regime, the Doppler and recoil effects are minimized. The wavelength of the optical lattice is 759 nm, which is called the magic wavelength,^[13] so the Yb atoms in such an optical lattice have an invariant $^1\text{S}_0$ – $^3\text{P}_0$ clock-transition frequency. Recently, 1D, 2D, and 3D optical lattices have been achieved with cold Yb atoms in our experiments. However, ^{171}Yb atoms have Zeeman sublevels in both the ground and the excited clock states; considering the polarization of the lattice light and the multiple sublevels in the clock states, for simplicity, a 1D optical lattice is better than a 2D or 3D optical lattice for making a clock,^[13] because in the 1D optical lattice, the polarization of the lattice light is spatially homogeneous. Therefore, in our experiment, we load the cold Yb atoms into a 1D optical lattice.

We use a Ti:sapphire laser pumped by a Verdi-18 laser (Coherent Corporation) to produce the 759-nm laser. The output power of the 759-nm laser is about 4 W. Since its frequency is far off resonance, the ^{171}Yb atoms will not be heated by the lattice light. We use a pair of lenses with 15-cm focal length to achieve a beam waist of about $30 \mu\text{m}$ at the center of the cold atomic cloud as shown in Fig. 2.

2.3. Clock-transition detection

In principle, the $^1\text{S}_0$ – $^3\text{P}_0$ clock transition of the ^{171}Yb atoms is double forbidden with spin and angular moments. Since the wavefunctions slightly overlap among the $^1\text{P}_1$, $^3\text{P}_1$, $^3\text{P}_0$ states, this transition is weakly allowed in reality, and its linewidth is ultranarrow, about 10 mHz. For observing the $^1\text{S}_0$ – $^3\text{P}_0$ clock transition, a 578-nm laser with a narrow linewidth is necessary. In our experiment, the 578-nm laser is generated by frequency summing a 1030-nm ytterbium-doped fiber laser with a 1319-nm Nd: YAG laser. The 578-nm laser is divided into three parts, and they are sent to the frequency-locking system, the optical frequency comb, and the cold Yb atoms, respectively. Especially for sending to the cold ^{171}Yb atoms, the 578-nm laser is exactly overlapped with the lattice

laser in space, and both waists are located at the atomic cloud center, and their polarizations are parallel, as shown in Fig. 2.

3. Experiment results

Figure 5 shows the timing sequence in our experiment. The first-stage cooling in the 399-nm MOT is on for 500 ms, the second-stage cooling in the 556-nm MOT is on for 100 ms after turning off the 399-nm MOT, Zeeman slowing laser, and atomic beam shutter at the same time. After the second-stage cooling, the cold Yb atoms, with a temperature of about $20 \mu\text{K}$, are loaded into the 1D optical lattice when all the lasers are off and the B -field is set to zero. After the cold atoms stay in the lattice for 20 ms, the 578-nm laser is turned on, and the cold Yb atoms in the $^1\text{S}_0$ ground state are excited into the $^3\text{P}_0$ excited state. After exciting the cold atoms for 50 ms, the 578-nm laser is off, and the 399-nm probe laser is turned on for measuring the population of the ground state after the excitation has been done. By changing the 578-nm laser detuning, we measure the dependence of the population of the ground state on the 578-nm laser detuning. In our case, the 759-nm laser is always on during the experiment.

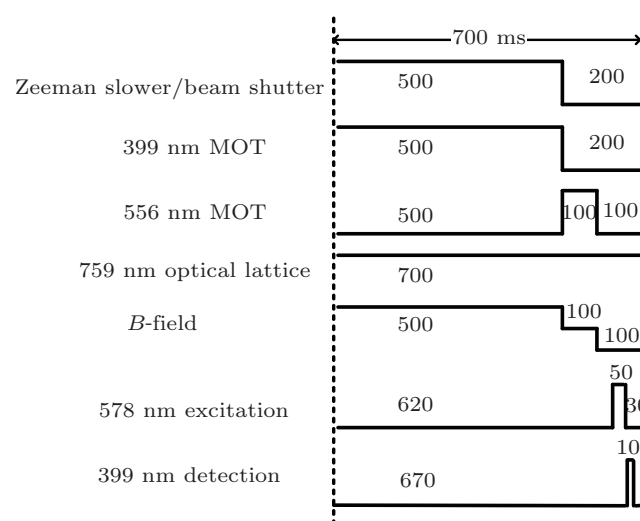


Fig. 5. Timing sequence of our experiment. The cycle time of the whole experiment is 700 ms. The 759-nm laser is always on during the whole experiment. The B -field is set at the high-low-zero three levels.

Figure 6 shows the experimentally-measured $^1\text{S}_0$ – $^3\text{P}_0$ clock-transition spectrum of ^{171}Yb atoms in the 1D optical lattice. When the 578-nm laser is far off the resonance of the clock transition, there is no excitation; since all atoms are in the $^1\text{S}_0$ ground state, the fluorescence signal induced by the 399-nm probe laser is the biggest. When the 578-nm laser is close to the resonance, some atoms at the $^1\text{S}_0$ ground state are excited to the $^3\text{P}_0$ excited state, and the fluorescence signal is reduced due to the decreasing ground-state population as shown in Fig. 6. Experimentally, a double-pass acoustic optical modulator (AOM) is used to scan and switch the 578-nm laser. The detuning of the 578-nm laser is changed with a

step of 0.1 kHz and a scanning range of 20 kHz. The data in Fig. 6 are the averages of four time measurements. The data are fitted with a Lorentz function, and the measured linewidth of the clock transition is 1.7 kHz. In Fig. 6, we can see only one peak because the magnetic field is near zero during the probing of the clock transition, so that all Zeeman sublevels of 3P_0 are degenerate, and all peaks in Fig. 6 are aligned. In our experiment, the residual magnetic field is less than 10 mG at the cold-atom cloud, inducing a few-Hz linewidth broadening and frequency shifting of the clock transition. In addition, the 578-nm laser linewidth is less than 10 Hz. Therefore, the observed linewidth of the clock transition is not dominated by the linewidth of the 578-nm laser at this moment. In the experiment, the 578-nm laser is sent to the cold ^{171}Yb atoms after going through the double-pass AOM. The frequency of the 578-nm laser is measured to be 518295680528.0 ± 2.9 kHz, and the frequency of the AOM corresponding to the resonance peak is 78031.3 ± 0.2 kHz in Fig. 6, therefore the resonance frequency of the $^1S_0-^3P_0$ clock transition of the ^{171}Yb atoms is 518295836590.6 ± 2.9 kHz. Compared with the latest data of the $^1S_0-^3P_0$ clock-transition resonance frequency of the ^{171}Yb atoms, 518295836590.865 kHz, which has been recommended as the secondary representation of the second by CIPM,^[14] the measured value is in agreement with the reported data within an uncertainty of 2.9 kHz.

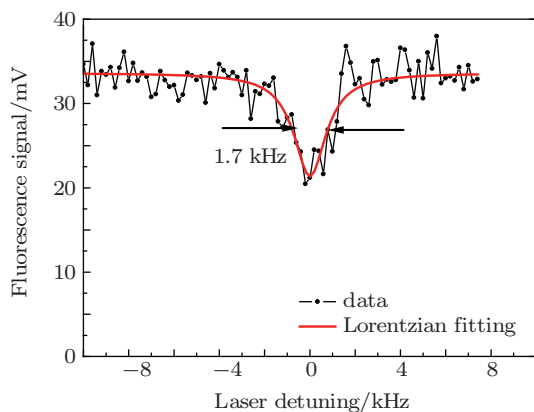


Fig. 6. (color online) Fluorescence signal induced by the 399-nm probe laser as a function of the 578-nm laser detuning. Fitted by a Lorentzian function, the linewidth of the spectrum is 1.7 kHz. The 578-nm laser power is set at 0.1 mW.

We also change the power of this excitation laser to obtain the linewidth variation with the 578-nm laser power as shown in Fig. 7. But when we further decrease the laser power, the linewidth does not approach zero as expected. That may be because the signal-to-noise ratio is getting worse due to the number of atoms fluctuating in each experimental cycle. Currently, we are going to improve the signal-to-noise ratio by using the normalization method. After finishing the 578-nm excitation followed by the ground-state population measurement, the atoms at the excited-state are pumped back to the ground

state by using the 649-nm and 770-nm lasers as shown in Fig. 1 and measured by the 399-nm probe laser. The total population of atoms during the clock-transition probe in this cycle is the sum of the measured two populations of atoms in the ground state. The excitation rate is the second-measured population divided by the total population. Therefore, the noise due to the number fluctuation will be ruled out from the signal, and then the power of the 578-nm excitation laser can be decreased, so that we may get the narrow linewidth of the clock transition of Yb atoms to develop an ytterbium optical clock.

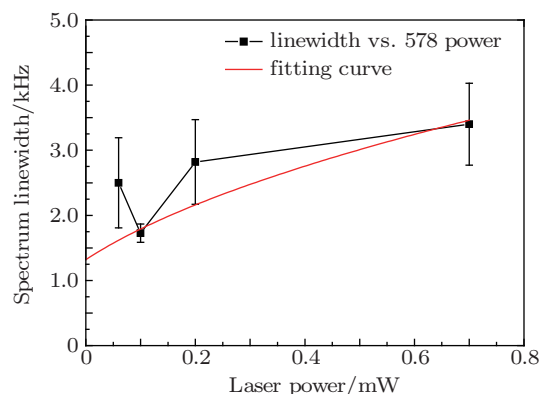


Fig. 7. (color online) Clock transition spectrum linewidth varies with the 578-nm laser power.

4. Conclusion

We have produced ultracold ^{171}Yb atoms with the temperature of 6 ± 3 μK . And the cold ^{171}Yb atoms have been loaded into an optical lattice with the wavelength of 759 nm. We have observed the clock transition spectrum of ^{171}Yb atoms in the 1D optical lattice with the excitation linewidth of 1.7 kHz. In the next step, we will improve the signal-to-noise ratio of the clock-transition spectrum with help of 649-nm and 770-nm lasers,^[15] hoping to realize closed-loop locking^[16–19] for the 578-nm clock laser and to measure the absolute $^1S_0-^3P_0$ clock-transition frequency of ^{171}Yb atoms more precisely.

References

- [1] Takamoto M, Hong F L, Higashi R and Katori H 2005 *Nature* **435** 321
- [2] Falke S, Schnatz H, Vellere Winfred J S R, Middelmann T, Vogt S, Weyers S, Lipphardt B, Grosche G, Riehle F, Sterr U and Lisdat C 2011 *Metrologia* **48** 399
- [3] McFerran J J, Yi L, Mejri S, Manno S D, Zhang W, Guéna J, Coq Y L and Bize S 2012 *Phys. Rev. Lett.* **108** 183004
- [4] Lemke N D, Ludlow A D, Barber Z W, Fortier T M, Diddams S A, Jiang Y, Jefferts S R, Heavner T P, Parker T E and Oates C W 2009 *Phys. Rev. Lett.* **103** 063001
- [5] Park C Y, Yu D H, Lee W K, Park S E, Kim E B, Lee S K, Cho J W, Yoon T H, Mun J, Park S J, Kwon T Y and Lee S B 2013 *Metrologia* **50** 119
- [6] Kohno T, Yasuda M, Hosaka K, Inaba H, Nakajima Y and Hong F L 2009 *Appl. Phys. Express* **2** 072501
- [7] Zhang J W and Yang D H 2007 *Chin. Phys. Lett.* **24** 1553
- [8] Jiang Y Y, Ludlow A D, Lemke N D, Fox R W, Sherman J A, Ma L S and Oates C W 2011 *Nat. photonics* **5** 158
- [9] Chou C W, Hume D B, Koelemeij J C J, Wineland D J and Rosenband T 2010 *Phys. Rev. Lett.* **104** 070802

- [10] Xu X Y, Wang W L, Zhou Q H, Li G H, Jiang H L, Chen L F, Ye J, Zhou Z H, Cai Y, Tang H Y and Zhou M 2009 *Front. Phys. China* **4** 160
- [11] Wang W L and Xu X Y 2010 *Chin. Phys. B* **19** 123202
- [12] Jiang H L, Li G H and Xu X Y 2009 *Opt. Express* **17** 16073
- [13] Katori H 2011 *Nat. photonics* **5** 203
- [14] <http://www.bipm.org/utis/common/pdf/CCTF19.pdf>
- [15] Cho J W, Lee H G, Lee S, Ahn J, Lee W K, Yu D H, Lee S K and Park C Y 2012 *Phys. Rev. A* **85** 035401
- [16] Yasuda M, Inaba H, Kohno T, Tanabe T, Nakajima Y, Hosaka K, Akamatsu D, Onae A, Suzuyama T, Amemiya M and Hong F L 2012 *Appl. Phys. Express* **5** 102401
- [17] Takamoto M, Hong F L, Higashi R, Fujii Y, Imae M and Katori H 2006 *J. Phys. Soc. Jpn.* **75** 104302
- [18] Ludlow A D 2008 *The Strontium Optical Lattice Clock: Optical Spectroscopy with Sub-Hertz Accuracy* (PhD thesis) (Colorado: University of Colorado)
- [19] McFerran J J, Magalhães D V, Mandache C, Millo J, Zhang W, Coq Y L, Santarelli G and Bize S 2012 *Opt. Lett.* **37** 3477